Journal of Statistical Physics, Vol. 22, No. 1, 1980

Enhanced $t^{-3/2}$ Long-Time Tail for the Stress–Stress Time Correlation Function

Denis J. Evans[1]

Received February 7, 1979; revised May 1, 1979

Nonequilibrium molecular dynamics is used to calculate the spectrum of shear viscosity for a Lennard-Jones fluid. The calculated zero-frequency shear viscosity agrees well with experimental argon results for the two state points considered. The low-frequency behavior of shear viscosity is dominated by an $\omega^{1/2}$ cusp. Analysis of the form of this cusp reveals that the stress–stress time correlation function exhibits a $t^{-3/2}$ "long-time tail." It is shown that for the state points studied, the amplitude of this long-time tail is between 12 and 150 times larger than what has been predicted theoretically. If the low-frequency results are truly asymptotic, they imply that the cross and potential contributions to the Kubo–Green integrand for shear viscosity exhibit a $t^{-3/2}$ long-time tail. This result contradicts the established theory of such processes.

KEY WORDS: Molecular dynamics; nonequilibrium; shear viscosity; frequency dependent.

1. INTRODUCTION

The discovery of long-time tails in the Kubo–Green time correlation functions is of fundamental importance to nonequilibrium statistical mechanics. This is underlined by their connection with the divergence of virial expansions for the transport coefficients and the fact that their form calls into question the very existence of Navier–Stokes hydrodynamics in two dimensions and Burnett hydrodynamics in three dimensions.[1]

In spite of the importance of long-time tails, experimental evidence for their existence is almost nonexistent.[2] The most graphic evidence for the slow decay of the Kubo–Green integrands for the hydrodynamic transport

[1] Ion Diffusion Unit, Research School of Physical Sciences, Australian National University, Canberra, Australia.

0022-4715/80/0100-0081$03.00/0

coefficients is still from computer simulation. It is well known that computer simulation evidence is consistent with a $t^{-3/2}$ long-time decay for the velocity autocorrelation function in three-dimensional systems.[3] The calculated coefficient has been shown to agree with theoretical predictions for both hard-sphere[3] and Lennard-Jones systems.[5]

As soon as we consider transport coefficients other than the diffusion coefficient, the computer evidence itself becomes much weaker. For shear viscosity, apart from the previous paper in this series,[7] there is no computer evidence for a $t^{-3/2}$ long-time tail for any three-dimensional system. Our knowledge of the $t^{-3/2}$ long-time tail for the stress–stress time correlation function rests upon the agreement of two-dimensional shear viscosity calculations with theory and the three-dimensional results for the velocity autocorrelation function.

For a two-dimensional system of hard disks Wainwright *et al.*[4] have shown that, asymptotically, the stress–stress time correlation function has t^{-1} form and that the coefficient of the kinetic–kinetic contribution has a magnitude in agreement with theory.[2,4,6] What is less well known is that Wainwright *et al.*[4] also observed behavior consistent with a t^{-1} long-time tail for the potential–potential and cross contributions to the time correlation function for the shear viscosity of hard disks. The consensus among theoreticians seems to be that only the kinetic–kinetic terms contribute a $t^{-d/2}$ long-time tail for shear viscosity in a d-dimensional system.[2,4,6] Indeed, Alder and Wainwright in their original explanation of the existence of long-time tails gave a theoretical argument for the fact that only kinetic–kinetic terms contribute such a tail for shear viscosity.[4] It is therefore assumed that the cross and potential terms must at times be beyond those accessible to the computer, and decay more rapidly than $t^{-d/2}$.

Intuitively this seems a little strange, since one usually expects that as times get longer, relaxation processes become slower. Computer evidence presented here suggests that at least for intermediate times, the potential and cross terms are decaying slowly ($-t^{-d/2}$). If theory is correct, then at longer times the decay of these terms must become more rapid than $t^{-d/2}$. This prediction raises such questions as: what processes, which presumably last out to intermediate times, prevent the early rapid decay of the potential and cross terms?

In this paper we present evidence for the $t^{-3/2}$ decay of the stress–stress time correlation function in a three-dimensional Lennard-Jones system. Our nonequilibrium molecular dynamics calculations are consistent with the $t^{-3/2}$ decay of the potential and cross terms. Indeed, if those terms did not exhibit $t^{-3/2}$ decay, then the amplitude of the kinetic–kinetic long-time tail is so small that we should never be able to see a $t^{-3/2}$ dependence of the stress–stress correlation function using our computational technique.

2. METHOD

Details of our algorithm for the calculation of the complex frequency-dependent shear viscosity coefficient have been published previously.[7] Briefly, the method uses a modified form of the Ashurst–Hoover[8] homogeneous shear algorithm. In the Ashurst and Hoover method oblique coordinate axes are used to allow the apparent motion of periodic images to produce a steady homogeneous shear. The shear viscosity η can then be calculated from the relation between stress P_{xy}, and strain rate $\partial u_x/\partial y$

$$P_{xy} = -\eta \, \partial u_x/\partial y \tag{1}$$

The stress is calculated from the standard expression

$$\mathsf{P} = \frac{1}{V}\left[\sum_i m[\mathbf{v}_i - \mathbf{u}(x_i)][\mathbf{v}_i - \mathbf{u}(\mathbf{x}_i)] + \frac{1}{2}\sum_{i \neq j} \mathbf{R}_{ij} \frac{\partial \Phi_{ij}}{\partial \mathbf{x}_0}\right] \tag{2}$$

where the summation is taken over atoms i within volume V and having mass, velocity, and position m, $\mathbf{v}_i$ and $\mathbf{x}_i$, respectively. It is assumed that the particles interact classically via a pair potential Φ_{ij} which depends solely on their relative position $\mathbf{R}_{ij} = \mathbf{x}_j - \mathbf{x}_i$.

A very important property of this method is the empirically discovered independence of the calculated viscosity coefficient of the size of the system simulated.[8,9] This is in marked contrast to equilibrium molecular dynamics, where not only must a larger number of time steps be used, but also larger systems have to be studied to prevent spurious results occurring as a result of the so-called "sound kink."[10] All the calculations described in this work used 108 particles.

The major difference of our technique from the Ashurst–Hoover scheme is the use of a least squares procedure at every time step adjust the velocity of every particle to that at the beginning of the next time step so that the strain rate is exactly linear and of the required rate.[7] This is quite a necessary modification for the calculation of a frequency-dependent shear viscosity.

The frequency-dependent calculation follows along the lines of the steady-state calculation except that a sinusoidal strain rate is used,

$$\partial u_x/\partial y = \gamma_0 \cos \omega t = \mathrm{Re}\{\gamma_0 e^{i\omega t}\} \tag{3}$$

For the strain rates γ_0 used here the system responds linearly in that the pressure tensor exhibits a sinusoidal time dependence with the same frequency as (but in general with a different phase to) the imposed strain. One then calculates the complex frequency-dependent shear viscosity as one would calculate the impedance of an electric circuit.

As has been shown in a previous paper,[7] this calculation is vastly more efficient than the corresponding Kubo–Green calculation, which calculates the frequency-dependent shear viscosity $\tilde{\eta}(\omega)$ from the formula[11]

$$\tilde{\eta}(\omega) = \int_0^\infty \eta(t) e^{i\omega t}\, dt \tag{4}$$

where the Kubo–Green integrand $\eta(t)$ is given as an equilibrium stress–stress time correlation function[12]

$$n(t) = (1/10kTV)\langle \mathring{\mathsf{P}}(0)^s : \mathring{\mathsf{P}}(t)^s \rangle \tag{5}$$

where $\mathring{\mathsf{A}}^s = \frac{1}{2}(\mathsf{A} + \mathsf{A}^T) - \frac{1}{3}\,\mathrm{tr}(\mathsf{A})\mathsf{I}$.

A nonequilibrium calculation begins with a 1000-timestep equilibration from the crystal. Zero-frequency calculations are then performed to discover the variation of effective viscosity with strain rate.[7,9] After identifying the "linear" region where the variation of shear viscosity with strain rate is less than the statistical fluctuations in the calculated viscosity, the frequency-dependent calculations are begun. At a typical frequency we use $\sim 15{,}000$ time steps, where the first two strain cycles are discarded. It typically takes two cycles for the pressure tensor to adjust to a steady sinusoidal pattern.

The potential used in this work was the standard Lennard-Jones (12, 6) potential for argon,

$$\Phi(r) = 4\epsilon[(\sigma/r)^{12} - (\sigma/r^6)] \tag{6}$$

with[13]

$$\epsilon/K = 119.8\ \mathrm{K}, \qquad \sigma = 3.405\ \text{Å}$$

All results are stated in reduced units, where the reducing parameters are ϵ, σ, and the argon atomic weight m.

Two state points were studied:

1. $T^* = 0.85$, $\rho^* = 0.76$.
2. $T^* = 2.28$, $\rho^* = 0.679$.

The first state lies on the coexistence curve for the Lennard-Jones fluid, relatively close to the triple point. The second is a supercritical, dense fluid state.

Table I summarizes the zero-frequency results for both state points. The zero-strain viscosities extrapolated using the Ree–Eyring formula[14] should be accurate to $\sim 4\%$. It can be seen that they are in good agreement with experiment. Recently Haynes[16] has suggested that in the region of our high-pressure state, the Michels *et al.*[15] data may underestimate the viscosity coefficient by approximately 10%.

Table I[a]

T^*	ρ^*	γ^*	η^*	t.s. $\times 10^3$	Δ^*
0.85	0.76	0.0333	1.787	22	0.008
0.85	0.76	0.0490	1.903	20	0.008
0.85	0.76	0.0989	1.967	10	0.008
0.85	0.76	0.1496	1.620	13	0.008
0.85	0.76	0.2475	1.634	10	0.008
0.85	0.76	0.4984	1.466	10	0.008
0.85	0.76	0.0	1.90 ± 0.05[b]		
0.860	0.7608	0.0	1.92[c]		
0.85	0.77	0.0	1.92[d]		
2.28	0.679	0.1002	1.307	24	0.002
2.28	0.679	0.1472	1.26	15	0.002
2.28	0.679	0.2025	1.15	25	0.002
2.28	0.679	0.2558	1.11	15	0.002
2.28	0.679	0.2985	1.20	20	0.002
2.28	0.679	0.4073	1.04	16	0.002
2.28	0.679	0.6003	1.13	11	0.002
2.28	0.679	0.0	1.27 ± 0.05[b]		
2.28	0.679	0.0	1.14[e]		

[a] Variables are reduced according to the Lennard-Jones parameters σ, ϵ, and the argon atomic mass m. $\Phi = 4\epsilon[(\sigma/r)^{12} - (\sigma/r)^6]$. $T^* = kT/\epsilon$, $\rho^* = \rho\sigma^3$, $\gamma^* = \gamma\sigma(m/\epsilon)^{1/3}$, $\eta^* = n\sigma^2(m\epsilon)^{1/2}$, $\omega^* = \omega\sigma(m/\epsilon)^{1/2}$, $t^* = t\sigma^{-1}(\epsilon/m)^{1/2}$.

[b] Estimate at zero strain rate.

[c] Hoover–Ashurst[8] estimate at zero strain rate.

[d] Experimental data.[16]

[e] Experimental data from argon.[15]

After determining the strain rate γ^* and the time step Δ^* that yield satisfactory zero-frequency results, the same values are used in the frequency-dependent calculations. At very high frequencies ($\omega^* \gtrsim 32$) it is necessary to use shorter time steps so that the frequency-dependent external forces do not vary appreciably within one integration time step. Periodically, checks are made at nonzero frequencies that the variation of the frequency-dependent viscosity with strain rate is still negligible.

3. RESULTS

Figure 1 shows the spectrum of the shear viscosity for $T^* = 0.85$, $\rho^* = 0.76$, giving the real and imaginary parts $\tilde{\eta}_R(\omega)$ and $\tilde{\eta}_I(\omega)$ as a function of frequency. These two components are not independent and they are

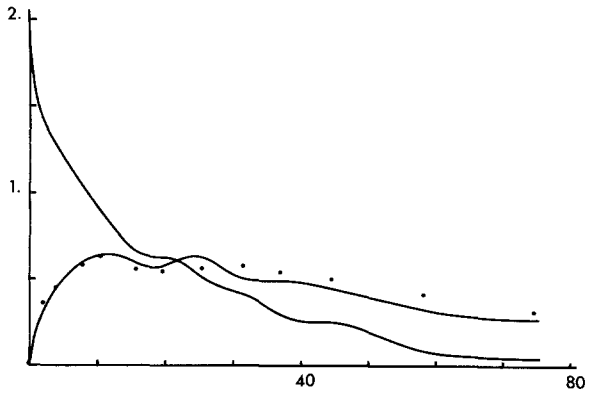

Fig. 1. The real and imaginary components of the shear viscosity of argon as a function of frequency. x axis is ω^*; y axis is $\tilde{\eta}^*(\omega^*)$. The points denote the Kramers–Kronig transform of $\tilde{\eta}_R(\omega)$. Here $\eta^* = \eta\sigma^2(m\epsilon)^{1/2}$, $\omega^* = \omega\sigma(m/\epsilon)^{1/2}$.

related by the Kramers–Kronig expression[17]

$$\tilde{\eta}_I(\omega) = \frac{2\omega}{\pi}\int_0^\infty \frac{\tilde{\eta}_R(\omega')}{(\omega')^2 - \omega^2}\, d\omega' \tag{7}$$

Figure 1 also shows the Kramers–Kronig transform (7) of $\tilde{\eta}_R(\omega)$. The agreement of the directly calculated imaginary component and the Kramers–Kronig transform of the real part is excellent, particularly at low frequencies. The difference of the two estimates for $\tilde{\eta}_I(\omega)$ gives an estimate of the numerical uncertainty of $\tilde{\eta}_I(\omega)$. The errors in the real component are thought to be roughly half those in $\tilde{\eta}_I(\omega)$.

We note that the Kramers–Kronig expression is an integral equation with a singular kernel. To avoid problems due to this singularity and due to the cusp in $\tilde{\eta}_R(\omega)$ at low frequencies, (7) was not used to calculate $\tilde{\eta}_I(\omega)$ directly. A double Fourier transformation was used instead. This method can still produce difficulties in the second transformation from $\eta(t)$ to $\tilde{\eta}_I(\omega)$. The reason for this is that the low-frequency cusp in $\tilde{\eta}_R(\omega)$ leads naturally to a long-time tail in $\eta(t)$. This would necessitate a very large number of discretization points for the Fourier transformation. These difficulties were avoided by using an analytic form for the low-frequency cusp in $\tilde{\eta}_R(\omega)$. Only deviations in $\tilde{\eta}_R(\omega)$ from this analytic form were transformed numerically. $\eta(t)$ was found as a sum of the numerically transformed deviations and the transform of the analytic part. The same splitting was used in the second transformation to obtain $\tilde{\eta}_I(\omega)$.

This splitting procedure is indeed very easy since, for $\omega^* < 15$, $\tilde{\eta}_R(\omega)$ takes the form

$$\tilde{\eta}_R(\omega) = \tilde{\eta}_R(0) - A\omega^{1/2} \tag{8}$$

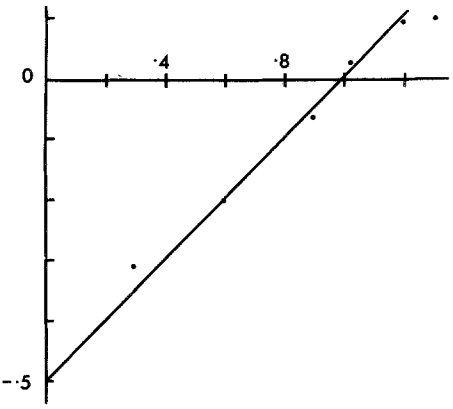

Fig. 2. Logarithmic plot of the low-frequency data from Fig. 1. The x axis is log ω^*; the y axis is $\log[\tilde{\eta}_R^*(0) - \tilde{\eta}_R^*(\omega^*)]$. Here $\eta^* = \eta\sigma^2(m\epsilon)^{1/2}$, $\omega^* = \omega\sigma(m/\epsilon)^{1/2}$

Figure 2 gives a logarithmic plot of $\tilde{\eta}(0) - \tilde{\eta}_R(\omega)$ against frequency. It shows that at low frequencies the data conform to (8) where $\tilde{\eta}_R^*(0) = 1.9$ and $A^* = 0.315$. This strong $\omega^{1/2}$ cusp in $\tilde{\eta}(\omega)$ was first seen by Evans in an analogous calculation for methane.[7]

The Taubernian theorems[18] imply

$$\lim_{t\to\infty} \eta(t) = \frac{A}{(2\pi)^{1/2}} t^{-3/2} \tag{9}$$

Thus we see that the coefficient of the long-time tail for the stress–stress time correlation function of a Lennard-Jones fluid at $T^* = 0.85$, $\rho^* = 0.76$ is given by $A^*/(2\pi)^{1/2} = 0.126 \pm 0.042$. For the second state point, $T^* = 2.28$, $\rho^* = 0.679$, we found very similar behavior. Again for reduced frequencies below 15, $\tilde{\eta}_R(\omega)$ exhibited an $\omega^{1/2}$ cusp. In this case the amplitude of the long-time tail is $A^*/(2\pi)^{1/2} = 0.0443 \pm 0.006$.

Recent mode coupling calculations of Bosse *et al.*[19] have predicted a resonance in $\tilde{\eta}(\omega)$ at twice the Einstein frequency for a Lennard-Jones fluid at the triple point. Apart from the $\omega^{1/2}$ cusp, we see very little structure; only a series of poorly resolved plateaus and troughs (Fig. 1). This contrasts with our earlier calculations for methane[7] and suggests that the resonance which was observed there was due to rotational rather than translational degrees of freedom. The position of the resonance in the methane calculation was ambiguous since the rotational and translational Einstein frequencies in methane at the state point studied are very close together.[20]

4. CONCLUSION

The theoretical expression for the long-time tail of the stress–stress time correlation function[1,2,4–6] is

$$\eta(t) \to \frac{kT}{15}\left(\frac{1}{8\pi t}\right)^{3/2}\left(\frac{7}{\nu^{3/2}} + \frac{1}{\Gamma^{3/2}}\right) \tag{10}$$

where ν is the kinematic viscosity and Γ is the acoustic damping coefficient. To the accuracy of the present calculations the term involving Γ may be neglected. In Table II we compare the magnitude of the long-time tails calculated from computer simulation with Eq. (10). We include in Table II the results on $\eta(t)$ from Levesque *et al.*[22] for a Lennard-Jones fluid at the triple point. Although Levesque *et al.* could not demonstrate that $\eta(t)$ has the asymptotic $t^{-3/2}$ form, they certainly saw a long-time tail in their equilibrium calculations. They characterized $\eta(t)$ by two exponentials. If we assume that at their longest time $\eta(t)$ is beginning to exhibit $t^{-3/2}$ dependence, then we obtain the value shown in Table II for the long-time tail at the triple point. For the state points considered here, (10) leads to values which are respectively 156 and 12 times smaller than the values calculated in our simulation! Furthermore, they have the opposite state dependence to that revealed in our calculations; our supercritical dense gas state has a weaker, rather than a stronger, long-time tail.

The origin of this discrepancy is not difficult to find. The theoretical expression predicts that the $t^{-3/2}$ long-time tail arises solely from kinetic–kinetic contributions to $\eta(t)$ [see Eq. (5)]. If we write

$$\eta = \eta_k + \eta_\Phi \tag{11}$$

where

$$p^k_{xy} = -\eta_k\, \partial u_x/\partial y, \qquad p^\Phi_{xy} = -\eta_\Phi\, \partial u_x/\partial y \tag{12}$$

and P^k and P^Φ denote the kinetic and potential parts of the pressure tensor, then for both state points considered here the results are completely dominated by P^Φ. If we let α be the ratio of P to P^k, then at the supercritical

Table II[a]

T^*	ρ^*	$A^*/(2\pi)^{1/2}$ simulation	$A^*/(2\pi)^{1/2}$ Eq. (10)
0.85	0.76	0.126 ± 0.042	8.0×10^{-4}
2.28	0.679	0.044 ± 0.006	3.8×10^{-3}
0.722	0.8442	0.672	4.0×10^{-4}

[a] $A^* = A\sigma^{1/2}m^{-1/2}\epsilon^{5/4}$.

state $\alpha = 5.5 \pm 2$ and for the other state $\alpha = 21.7 \pm 7$. The relatively large errors in α arise because of the smallness of η_k relative to η, which we assume is known to $\sim 3\%$. At the triple point Ashurst and Hoover[9] have shown that $\alpha = 42$. As far as is known to the author, no exact connection between η_k, η_Φ, and the analogous decomposition into kinetic–kinetic, cross, and potential–potential terms for the Kubo–Green integrands is known. Ashurst and Hoover have pointed out[25] that in the Enskog approximation the kinetic–kinetic and half the cross term comprise η_k and the potential–potential and half the cross term form η_Φ. Although this prediction may not be exact, it seems safe to assume from our results that even if *all* the kinetic–kinetic term decayed as $t^{-3/2}$, its contribution to $\eta(t)$ is simply too small to explain our results. Our results therefore imply a long-time tail for the potential and cross terms of the stress–stress time correlation function. Figure 2 shows that the decay of these terms is consistent with a $t^{-3/2}$ dependence.

Finally we must mention the fact that occasionally conjectures have been made about the accuracy of the Kubo–Green expressions for the hydrodynamic transport coefficients. It has been suggested that the hydrodynamic transport coefficients are given by the Kubo–Green expressions *minus* the contribution from the $t^{-3/2}$ long-time tail (see Refs. 22 and 24 for discussions of this point). We believe that our simulations have demonstrated that this conjecture is wrong. Nonequilibrium molecular dynamics closely mimics experiment, and as our frequency-dependent calculations show, the zero-frequency transport coefficients, which agree closely with experiment, do have contributions from an apparently $t^{-3/2}$ long-time tail.

Note Added. After this work was submitted for publication Wood and Erpenbeck sent us results of some new calculations of $\eta(t)$ for hard spheres obtained using equilibrium molecular dynamics.[26] Their early results seem to support the main points made by this paper. They find a $t^{-3/2}$ tail for both the cross and potential contributions to $\eta(t)$ and that the total $t^{-3/2}$ tail for $\eta(t)$ is approximately two orders of magnitude greater than theory predicts for the state point they studied.

REFERENCES

1. J. R. Dorfman and H. van Beijeren, The Kinetic Theory of Gases, in *Statistical Mechanics, Part B*, B. J. Berne, ed. (Plenum, 1977), p. 65.
2. Y. Pomeau and P. Resibois, *Physics Reports* **19**:63 (1975); see p. 126.
3. B. J. Alder and T. E. Wainwright, *Phys. Rev. A* **1**:18 (1970).
4. T. E. Wainwright, B. J. Alder, and D. Gass, *Phys. Rev. A* **4**:233 (1971).
5. D. Levesque and W. T. Ashurst, *Phys. Rev. Lett.* **33**:277 (1974).
6. M. H. Ernst, E. H. Hauge, and J. M. J. Van Leeuwen, *Phys. Rev. Lett.* **25**:1254 (1970); *J. Stat. Phys.* **15**:7 (1976).
7. D. J. Evans, *Molec. Phys.* **37**: 1745 (1979).

8. W. T. Ashurst and W. G. Hoover, in *Theoretical Chemistry Advances and Perspectives, Vol. I*, H. Eyring and D. Henderson, eds. (Academic Press, 1975).
9. W. T. Ashurst and W. G. Hoover, Sandia Report SAND 77-8614.
10. B. J. Berne, *Faraday Symposium* **11**:48 (1977).
11. J. P. Hansen and I. R. McDonald, *Theory of Simple Liquids* (Academic Press, 1976).
12. D. J. Evans and W. B. Streett, *Molec. Phys.* **36**:161 (1978).
13. L. Verlet, *Phys. Rev.* **159**:98 (1967).
14. F. H. Ree, T. Ree, and H. Eyring, *Ind. Eng. Chem.* **50**:1036 (1958).
15. A. Michels, A. Botzeau, and W. Schuurman, *Physica* **20**:1141 (1955).
16. W. M. Haynes, *Physica* **67**:440 (1973).
17. F. C. Brown, *The Physics of Solids* (Benjamin, 1967), Appendix I.
18. G. Doetsch, *Guide to the Applications of Laplace Transforms* (Van Nostrand, 1961).
19. J. Bosse, W. Gotze, and M. Lucke, *Phys. Rev. A* **17**:434 (1978).
20. S. Murad, D. J. Evans, K. E. Gubbins, W. B. Streett, and D. J. Tildersely, *Molec. Phys.* **37**: 725 (1979).
21. M. H. Ernst, E. H. Hauge, and J. M. J. van Leeuwen, *Phys. Rev. A* **4**:2055 (1971).
22. D. Levesque, L. Verlet, and J. Kurkijarvi, *Phys. Rev. A* **7**:1690 (1973).
23. W. W. Wood, in *The Boltzmann Equation*, E. G. D. Cohen and W. Thirring, eds. (Springer-Verlag, 1973), p. 468.
24. R. Zwanzig, in *Statistical Mechanics*, S. A. Rice, K. F. Freed, and J. C. Light, eds. (Chicago University Press, 1972), p. 241.
25. W. T. Ashurst and W. G. Hoover, *Phys. Rev. A* **11**:658 (1975).
26. W. Wood, private communication.